

RC1:

You describe an interesting 'longer term' link between earthquake occurrence and massive periglacial surface processes. I would mainly recommend a general (and professional) English review, and adding some lines about the physical relationship between the seismic and (peri) glacial processes. It is also important to highlight the relatively large distance (if I see well) between the 1950 Assam earthquake epicenter (or distance to activated fault) and the glacier valley.

- **Author's response:**

Thanks for your advice! The full text has been reviewed by native English speakers to enhance the manuscript's readability and professionalism.

As for the physical relationship between the seismic and (peri) glacial processes, we have already had a supplementary discussion in Section 6.1:

Strong ground vibrations caused by earthquakes can intensify cracking within the ice/rock mass, ultimately leading to the formation of substantial failure surfaces (Kilburn and Voight, 1998). Additional loading by earthquakes and coseismic-ice/rock avalanches could destruct the englacial conduit and subglacial drainage system. These changes can cause dynamic alterations to the glacier's thermal sensitivity, exacerbating its instability (Zhang et al., 2022). As critical solid material sources, these highly active ice/rock masses caused by seismic disturbance are prone to avalanches, calving, detachment and remobilization to form glacial debris flows (Deng et al., 2017; Zhang et al., 2022).

The epicenter of the 1950 Assam earthquake is approximately 195 kilometers away from the ZLL Valley. Notably, this seismic event not only triggered the glacier surge-debris flow chain but also incubated the 1953 debris flow in Guxiang Valley, approximately 50 kilometers northeast of the ZLL Valley. Although the Guxiang debris flow did not occur on the same day as the earthquake, the 1950 earthquake induced co-seismic avalanches, ice falls, and rockfalls of an unprecedented scale upstream of Guxiang Valley. These events contributed a substantial volume of loose material, which subsequently led to the 1953 debris flow.

- **Author's changes in manuscript:**

The manuscript has been reviewed by native English speakers to enhance the manuscript's readability and professionalism.

we have already had a supplementary discussion about the physical relationship between the seismic and (peri) glacial processes in Section 6.1.

we have emphasized the large-distance characteristics of the 1950 earthquake and the ZLL Valley in the first paragraph of section 6.1, and marked the location of the earthquake in Figure 1b.

RC2:

Hu and co-authors present an analysis of periglacial debris flows in a small catchment draining the Namche Barwa massif in the Himalaya using historical and modern remote sensing applications. I have some suggestions for improvements. In particular, I am not convinced by the discussion about the causes for the debris flows.

1. **Motivation of the paper:** First I suggest to sharpen the motivation of the paper. According to the introduction (L61 ff), “little is known about the roles the extreme hazards play in incrementing sediment erosion, transportation, and the control of the hazards between tectonic and climatic factors.” I actually do not quite understand what is meant here.

- **Author's response:**

Recent observations indicate that episodic debris flows are predominately responsible for sediment transport from steep lands to rivers and channel erosion, being a major agent in landscape evolution in high mountain areas (Anderson et al., 2015; Kober et al., 2012; Lancaster and Casebeer, 2007; McCoy et al., 2013). Lin et al. (2006) presented that it could last for more than 10 years after the Chi-Chi earthquake. Cui et al. (2011) predicted that the effect of Wenchuan earthquake on post-quake debris flows would last for 10-20 years, while Huang (2011) predicted that it would be from 20 to 25 years. Recent publications demonstrate that only ~ 30% portion of coseismic sediment has been evacuated by debris flows and fluvial transport 12 years after the

Wenchuan earthquake (Dai et al., 2021), and the fine-grained landslide sediment mobilized by the earthquake may stay in the affected river catchments as long as a century (Wang et al., 2015). Until now, most of previous studies have focused on the residence time and transport of earthquake-triggered landslide sediment at an orogenic scale in no-glacierized environments (Dadson et al., 2004; Dai et al., 2021; Parker et al., 2011; Wang et al., 2015). Little attentions are paid on the sediment evacuation progress by post-seismic debris flows at a catchment in glacierized environments owing to relatively low likelihood of debris flows and absence of long-term site-specific data. Consequently, this paper is driven by the motivations:

- To describe how strong earthquakes and warming events escalate debris flows and associated sediment transport within small alpine watersheds.
- To clarify how long the effects of an earthquake on periglacial debris flows at a glaciated catchment.
- To examine the roles that climate and tectonics play in the development of extreme hazards in the tectonically active and climate-sensitive region of southeastern Tibet.

The reviewer's meticulous examination has highlighted an issue with our initial phrasing, which led to ambiguity. To clarify, we deleted the sentence and changed it with: " Little attentions are paid on the sediment evacuation progress by post-seismic debris flows at a catchment in glacierized environments owing to relatively low likelihood of debris flows and absence of long-term site-specific

data."

- **Author's changes in manuscript:**

We have revised this sentence.

2. **Second, it is not made clear in the following text how that knowledge gap is addressed by the study. Questions that would be good to answer in the introduction are: Why was that particular study area chosen? How do the approaches advance the gap that you are proposing? In the discussion or conclusion, you can also come back to that point.**

- **Author's response:**

As mentioned above, we want to study the sediment evacuation process dominated by debris flows in glacierized environments. In order to investigate the long-term effects of earthquakes on sediment evacuation in a glaciated catchment, we select the Zelunglung catchment, a tributary of the Yarlung Tsangpo river in southeastern Tibet that has large areas of temperate glaciers and disturbed intensely by the Ms 8.5 earthquake in 1950. Moreover, the catchment has long-term remote sensing imagery for interpreting glacier changes and associated debris flows and relatively well-documented records of at least four historical periglacial debris flows in 1950, 1968, 1972, and 1984 since the 1950 Assam earthquake.

- **Author's changes in manuscript:**

We added the explanation in the last paragraph of the Introduction.

3. Methodology: I do not quite understand how you can take the non-vegetated area as a proxy for debris flow volume (e.g. L135). To get a volume from an area, I believe you need some estimate of thickness. How do you get that?

● **Author's response:**

We appreciate the reviewer's valuable comment. As you pointed out, accurate estimation of debris flow volume is hindered by the lack of sediment thickness data. The sediment volume of debris flow may be influenced by various factors, such as fan area, average fan slope and average channel (e.g. Stoffel (2010)). Nevertheless, conducting a long-term time series analysis since 1950 presents challenges in acquiring adequate data for estimating sediment volume over the past century. Borehole method can give the accurate estimation of thickness, but is too expensive for our study. Consequently, this study employs an approximate alternative approach, wherein the fluctuation in debris flow volume is inferred from changes in the area of the accumulation fan. Actually, many previous studies consider debris flow volume is empirically a function of the accumulation area (e.g. Iverson et al. (1998)). It is crucial to underscore that our emphasis lies not on the absolute volume of debris flows but on their relative trends.

● **Author's changes in manuscript:**

We made no changes to this part of the manuscript.

4. Causes of debris flows: First the discussion of causes for the debris flows is a bit confusing to me. In the abstract you write that the four events 1950 – 1984 were legacies of the 1950 Assam earthquake. The suggested link between the 1950 Earthquake and the 1950 debris flow seems solid (as per Fig. 15). The suggestion that the other events were also preconditioned by that earthquake seems less obvious to me. Is the only evidence that none of the other earthquakes could have caused the debris flows (L381ff)? What about other possible triggers, such as an extreme precipitation events? I am by no means an expert, but the argument for the influence of the 1950 earthquake on later debris flows doesn't seem very convincing to me. By the way, in the discussion (L381ff), it did not become clear that you actually suggest that the 1950 – 1984 events were all triggered by the earthquake. I only got that from the abstract.

● **Author's response:**

The influence of a large earthquake on debris flows is a long lasting process, with variable durations of impact in different studies (Dai et al., 2021). For instance, following the Wenchuan earthquake, Tang et al. (2009) suggest a debris flow activity span of 5 to 10 years, whereas Cui et al. (2008) propose 20 to 30 years. Xie et al. (2009) indicate the possibility of strong debris flow activity persisting for 10 to 30 years, or more. Essentially, the above statement pertains

to the active duration of earthquake impacts on the loose source of debris flow channels. But, when the earthquake's effects is negligible, debris flow frequency-magnitude will resume to pre-quake level. Pre-1990 debris flow events as indicated by Figure 12d (in the Figures part of this document), represent a legacy of the 1950 earthquake. Of course, the post-seismic debris flows maybe directly triggered by extreme precipitation or temperature fluctuation. But the instability of the glacier/materials caused by the great earthquake is not negligible. Prior to 1990, NVA exhibited a consistent decline, whereas afterward, it displayed significant fluctuation and even a slight upward trend. This implies that the aftermath of the 1950 earthquake persisted until 1990, after which debris flow resumed activity on a relatively minor scale, influenced by climatic factors. Despite the occurrence of several small earthquakes preceding the events of 1968 and 1984 as noted by L381ff, these earthquakes were not captured by the Keefer curve considering magnitude and distance (figure 13 in manuscript), suggesting their minimal influence on the debris flow events.

- **Author's changes in manuscript:**

We supplement the above in Section 6.1.

5. **Also, in the abstract you say that “recent warming events drove the 2020 event”. And you start your discussion stating that either earthquakes or climate change increase the occurrence of debris flows. I do not think you have evidence to say that unless you have a much**

longer time series. Lets assume the null-hypothesis that debris flow events occur randomly within some average recurrence interval. With the few events you study here, I would challenge you to show that the distribution of earthquakes is statistically distinguishable from a random occurrence. Similarly, I would challenge that a single debris flow after a single warming episode is evidence enough to conclude this flow is caused by the warming. I suggest to formulate these links much more carefully and “suggest” a link.

- **Author's response:**

We appreciate the valuable suggestion provided by the reviewer. The assumption of temporal random distribution of debris flows is probably right at an orogen scale. For a specific catchment, the debris flows are not random temporally, but controlled by earthquakes or climate events. That is confirmed by the 1999 Chi-chi earthquake and the 2008 Wenchuan earthquake. Whether earthquakes and climate change will definitely increase the occurrence of glacial debris flow is indeed to be further studied, but for the southeast Tibet region where ZLL is located, this seems to be based on evidence. For example, the Assam earthquake in 1950 caused frequent debris flow activities in Guxiang Valley for decades(Du and Zhang, 1981), and the increase of glacier ablation under the influence of climate change in the past 20 years has promoted the debris flow in Tianmo Valley (Deng et al., 2017) and Sanggu Valley (Wang et al., 2023). Therefore, in order to ensure objectivity, we change the relevant

statement to: "It is evident that either earthquakes or climate change may increase the occurrence of periglacial debris flows and their sediment yield in southeastern Tibet."

Figure 12 illustrates a notable decrease in rainfall since 2000, alongside an increase in temperature, with a particularly sharp rise in 2018. Remarkably, this pattern closely resembles the fluctuation of NVA. Although extreme rainfall may also induce debris flows, from the observation data of the Linzhi meteorological station (29.568° N, 94.467° E), the average maximum and minimum temperature from 15 August to 14 September in 2020 were 27 °C and 13 °C and the daily rainfall in this period ranged from 0 to 17.5 mm/d. According to an eyewitness video at 18:55 on 10 September 2020, the steel bridge deck was dry, which indicated that the precipitation was light on the event day (Peng et al., 2022). Therefore, combining the long-term climate trend and the daily value data before the event, we believe that the debris flow is caused by warming.

- **Author's changes in manuscript:**

we have added relevant references to the sentence: "It is evident that either earthquakes or climate change may increase the occurrence of periglacial debris flows and their sediment yield in southeastern Tibet".

We have added some sentences describing the weather in the month of the debris flow in the last paragraph of section 6.1.

6. Line comments:

L105: Just visually. Fig. 2 doesn't particularly look like precipitation is increasing at all. How did you calculate that increase?

● **Author's response:**

As depicted in Figure 2b, the precipitation at Linzhi Station exhibited significant fluctuations from 2000 to 2021. The linear regression analysis revealed a minimal growth rate of rainfall, specifically 0.065 mm/year, which was not readily discernible from the raw data. To enhance clarity, we have included fitted trend lines for both temperature and precipitation in figures 2a and b.

● **Author's changes in manuscript:**

We replaced the figure with a new one.

L132: I would start the methods section with a summary sentence of the measurements that you are trying to make.

● **Author's response:**

Thanks for your suggestion. We changed the structure of this section. We set the field surveys as a part of the methodology, and divided the original methodology section into two parts, they are NVA interpretation and Drone image interpretation. And we add a summary paragraph at the beginning of the sub methods section, as described below:

The study utilizes a combination of field surveys, aerial drone photography, and satellite imagery analysis to investigate debris flow events in the Zelunglung region. High-resolution orthoimages and digital surface models are generated

to assess terrain changes, while non-vegetated area (NVA) serves as a proxy for sediment volume for time series analysis. The integration of these methods offers a detailed insight into the debris flow history and its influencing factors.

- **Author's changes in manuscript:**

We changed the structure of this section. We set the field surveys as a part of the methodology, and divided the original methodology section into two parts, they are NVA interpretation and Drone image interpretation. And we add a summary paragraph at the beginning of the methodology.

L159ff: I suggest to move the entire section on glacier changes before the methods. This is not your work as far as I understand, so it's a bit odd to have that as part of the other results. You could move it together with the study area section

- **Author's response:**

Thanks for your suggestion, we have integrated this section into the study area section.

- **Author's changes in manuscript:**

We have integrated this section into the study area section, and meanwhile, we merged the figure 3 into figure 1c.

L336: Can you explain where the interpretation of “some kind of dilute or hyper-concentrated flow” comes from?

- **Author's response:**

Thank you for your review. We apologize for the oversight; this sentence was part of our original draft and was mistakenly left in, leading to a misunderstanding. We have now deleted it.

- **Author's changes in manuscript:**

We deleted the sentence.

L351ff: A lot of that section reads like a discussion. I suggest to move it there.

- **Author's response:**

Thanks for your suggestion, we moved the last 2 paragraph this section to the discussion section (new section 6.1), and named it with "The dominant factor for debris flows and sediment yield". As a consequence, the section 6.2 was renamed to "The future risk".

- **Author's changes in manuscript:**

We moved the last 2 paragraph this section to the discussion section (new section 6.1), and named it with "The dominant factor for debris flows and sediment yield". As a consequence, the section 6.2 was renamed to "The future risk".

Another note on this paragraph: You write of three surges (L168) but then only explicitly note two of them (L169ff and L172ff). I guess the third surge

is the one you describe in L179? Can you make that explicit?

- **Author's response:**

Thanks for your suggestion. Yes, the third surge occurred in 1984, and we wrote this date in the article.

- **Author's changes in manuscript:**

We have identified third surge in the article.

For all of the figures with geographic reference, it has to be clear where they are from with respect to the region. Figure 1 is missing a regional overview map. It was unclear to me where Figures 4 – 6 are taken within the study area or what extent Figs. 8-11 have. You can either mark their positions in Figure 1, or have little insets with every figure that show where in the study area that figure/picture is located. Also, not all figures have information on orientation and, if relevant, scale (e.g. Fig. 4-6. 7c&d, Photo of Fig. 9 missing north arrow etc.)

- **Author's response:**

Thanks for your suggestion. We added a regional overview map, and designated as Figure 1a. The interrelations among the sub-figures of Figure 1 are depicted using differently colored rectangular boxes. The camera's view direction of Figure 1d is marked with the orange arrow Figure 1c.

For extents of other independent images or view angle direction of photos in

the paper, we also marked them with rectangular boxes or arrows of different colors in Figure 1c. The details are as follows:

1. The scope of Figure 3a is indicated by a blue box in Figure 1c, whereas the extents of Figures 3b to 3f are delineated within Figure 3a itself.
2. The viewing angle in Figure 4 corresponds to the direction of the rose-red arrow in Figure 1c.
3. The viewing angle of the 3D satellite image in Figure 5a is aligned with the direction of the green arrow in Figure 1c.
4. The viewing angle directions for the photographs in Figures 6c and 6d are marked by black and red arrows, respectively, in Figure 1c.
5. We have standardized the display ranges of Figures 7, 8-a1, and 10 for uniformity, as indicated by a rose-red box in Figure 1c.
6. Given the constrained space in Figure 1c, the scope of Figure 9 is delineated using black boxes in Figure 7b.
7. The scope of Figure 11 is demarcated by a green box in Figure 1c

We have added north arrow in figures 1d, 3, 4, 5, 6c, 6d and 11. We have add scalebar in figures 3, 6a-b and 11. Add we also marked the view angle direction of photos 4, 5, 6c and 6d in figure 1c by rose-red, green, black and red coloured arrows, respectively.

● **Author's changes in manuscript:**

We changed the figures according to the comments, and made corresponding

modifications in the captions.

Figure 1: The yellow text in panels b&c and the white text in panel a was hard to read on my printout.

- **Author's response:**

Thanks for your suggestion. We have re-evaluated the text within the Figure 1 and implemented changes to the text color scheme. Additionally, we introduced a mask behind the text to enhance its contrast against the background, thereby improving legibility.

- **Author's changes in manuscript:**

We replaced the figure with a new one.

Figure 4: The year numbers are a bit hard to see against the grey background

- **Author's response:**

Thanks for your suggestion. We changed all the texts in to yellow to make it easier to recognize.

- **Author's changes in manuscript:**

We replaced the figure with a new one.

Figure 6: There is no explanation in the figure or caption what T1-T2 are. Even if it is quite obvious, it would be good to define explicitly. The North

Arrow and scale-bar is really hard to see.

- **Author's response:**

Thanks for your suggestion. Consequently, we have included explanations for T1 and T2 within the figure's caption. The North Arrow and scale bar in Figure a have been redesigned to enhance their visibility. Additionally, we have indicated the viewing angle direction of Figure b using a green arrow in Figure a.

- **Author's changes in manuscript:**

We replaced the figure with a new one, and included explanations for T1 and T2 within the figure's caption.

Fig 8c: The person as scalebar is really hard to see

- **Author's response:**

We have changed the photo in Figure c, which the person as scalebar in it is clearer. Red arrows have been employed to indicate the viewing angle direction of the photograph in Figure c, and the heights of the person have been annotated.

- **Author's changes in manuscript:**

We replaced the figure with a new one.

Figure 12: Can you give some more information in the figure caption about where the 'on-site' sample is and when the sample was taken?

- **Author's response:**

The 'on-site' sample was taken at the alluvial fan on September 11, 2020 (the day after the 2020 event). We have included this figure into figure 8, and numbered it as figure 8d. The location of the on-site sample was marked in figure 8a-1.

- **Author's changes in manuscript:**

We added the information in section 3.2.1 "Field surveys".

RC3:

1. The manuscript "Variation of sediment supply by periglacial debris flows at Zelunglung in the easter syntaxis of Himalayas since 1950 Assam Earthquake" by Hu et al., describes the occurrence of five debris flows that impacted the Zelunglung alluvial fan using a combination of field surveys, historical aerial imagery, and UAV flights. The manuscript contributes with observations on long-term changes in vegetation at the alluvial fan interpreted as a proxy for debris flow activity at the catchment. The manuscript aims to estimate relative qualitative debris flow activity compared to the 1950 event. Also, a detailed description of the 2020 debris flow event is presented using UAV photogrammetry. The authors discuss the results considering seismic activity, the Zelunglung glacier surge dynamics, and precipitation and air temperature. The manuscript exemplifies the complex interactions between tectonic and climate in debris flows triggering factors in glaciated areas. Despite the presented remote sensing interpretation, field observation, and literature review, further considerations are needed to strengthen the conclusions, particularly the conclusion referring to the influence of the 1950 earthquake in further debris flows until 1990.

- **Author's response:**

Thank you for your appreciation! As you mentioned, the debris flow activity in

glaciated areas is more complex than in non-glaciated areas. Our case study attempt to shed light on how tectonic and climatic factors influence sediment evacuation processes via debris flows. Lin et al. (2006) presented that it could last for more than 10 years after the Chi-Chi earthquake. Cui et al. (2011) predicted that the effect of Wenchuan earthquake on post-quake debris flows would last for 10-20 years, while Huang (2011) predicted that it would be from 20 to 25 years. Recent publications demonstrate that only ~ 30% portion of coseismic sediment has been evacuated by debris flows and fluvial transport 12 years after the Wenchuan earthquake (Dai et al., 2021), and the fine-grained landslide sediment mobilized by the earthquake may stay in the affected river catchments as long as a century (Wang et al., 2015). Compared with the 1999 Chi-chi earthquake and the 2008 Wenchuan earthquake, the influence period of the 1950 earthquake is longer. We think the earthquake effects last longer in glaciated areas.

- **Author's changes in manuscript:**

We added a sentence in the third point of the conclusion “”.

2. **The presented historical aerial imagery is a valuable source of information that could be explored to strengthen the manuscript. For example, if available, the source and affected area of the historical periglacial debris flows (1950,1968,1972,1984) could be identified.**

- **Author's response:**

We show our gratitude to the reviewers for their valuable feedback. Regrettably, we lack the necessary resources to support this research. Obtaining high-resolution images of both the source and affected areas, especially from immediately before and after the events, presents significant challenges due to the lack of advanced satellite remote sensing technology during that time period. Apart from the 1972 event, the occurrence of the other three events is well-documented in previous literature (as we quoted in my manuscript).

- **Author's changes in manuscript:**

We made no changes to this part of the manuscript.

3. I missed in the manuscript a clear explanation about why you consider that the 1950 earthquake has a stronger influence than the glacier surges in the triggering of the debris flows after 1950 and, therefore, impacting the vegetation changes between 1950 and 1990 (line 484). In lines 187-188, it is stated that the debris flows were triggered by the glacier instability. Also, the 1950 debris flow coincides with a glacier surge.

- **Author's response:**

As Zhang and Shen (2011) have stated: "The Chayu violent earthquake (Ms 8.5, on Aug 15, 1950) evoked Zelongnong glacier surge (Zhang 1985). After the rapid motion the ice cube carrying a mass of solid matter moved to the lower reaches. Ice block thawed and evolved into debris-flows during this process, a

great deal of ice block and grit deposited at the convergence mouth." Therefore, the events triggered by the 1950 earthquake constituted a chain reaction of glacier surge and debris flow, wherein the glacial process was integral to the debris flow mechanism. The impact of such a seismic event does not dissipate suddenly. Pre-1990 debris flow events, in our view, represent a legacy of the 1950 earthquake. While their occurrence may have been directly triggered by glacial advancement or extreme precipitation, the root cause is the continued under stability of the glacier/materials caused by the great earthquake. Prior to 1990, NVA exhibited a consistent decline, whereas afterward, it displayed significant fluctuation and even a slight upward trend. This implies that the aftermath of the 1950 earthquake persisted until 1990, after which debris flow resumed activity on a relatively minor scale, influenced by climatic factors.

- **Author's changes in manuscript:**

We explained more details in section 6.1.

We have modified the expression of lines 187-188: Four large-magnitude debris flows accompanied by glacier instability occurred in 1950, 1968, 1973, and 1984.

- 4. The photo interpretation from Planet Lab images shows an ice-rock residual under the detachment area of the 2020 debris flow. The authors conclude that the entrained volume is at least 16 times the initiated volumes (line 227), consistent with the 1.14 Mm^3 previously presented by Peng et al., (2022). This is highly relevant for the**

calibration of Debris Flow models.

- **Author's response:**

Thank you for your suggestion! Yes, this data can be used to calibrate ice-rock avalanche and debris flow models.

- **Author's changes in manuscript:**

No Change.

5. The proposed methodology involved a considerable amount of remote sensing data manual interpretation and general information on the uncertainty of the manual mapping of non-vegetation areas was given. Regardless, I missed a short sentence on the reconstruction of the DSM from the UAV surveys (e.g., software use, ground control points, alignment), and the uncertainty on the elevation change that propagates to the presented volumes (line 346).

- **Author's response:**

The reconstruction and differencing of DSMs are carried out in Pix4DMapper and Arcmap10.8. Since we did not deploy ground control points during drone photography, we generated DSM and DOM of September 9 in Pix4DMapper, and then selected 20 relatively stable points that were not affected by debris flow events as control points in Arcmap with DOM of September 9 as reference. These control points were then used in Pix4DMapper to generate the September 11 DSM and DOM.

To determine the uncertainty for our UAV DSMs of difference (DoD) differencing result we follow methods outlined in Shugar et al. (2021). We identified a series of fifteen stable areas on old debris flow terraces adjacent to the valley floor (Mainly roads and unseeded farmlands) and retrieved the standard deviation of DoD values within these areas and used these to estimate a two-sigma DoD uncertainty. The uncertainty was ± 0.493 m.

- **Author's changes in manuscript:**

We have included a description of this in section 3.2.3 "Drone image interpretation".

The manuscript is well structured and the figures are illustrative.

6. Line comments:

Line 130-131: Did you present results on the surveys in 2021 and 2022 in this manuscript?

- **Author's response:**

We conducted three field surveys, as described in lines 68-69 of the manuscript. The initial two were scheduled one day before and one day after the 2020 event, on September 9 and 11, 2020, respectively. Predominantly, these surveys involved drone photography before the disaster and included drone photography, measurements, and sampling in the post-disaster assessment. The third survey took place on December 21, 2022, and was specifically designed to capture aerial photography of the ZLL basin's upper reaches, an area

inaccessible in the prior surveys due to adverse weather conditions. The outcomes of the 2022 survey are detailed in Figures 1d, 4, and 6c, providing insights into the upstream channel and the debris flow initiation zone. We did not execute a field survey in 2021. We offer our apologies for any confusion that our initial errors may have caused.

- **Author's changes in manuscript:**

We retraced field survey timeline in section 3.2.1.

Figure 4: Can you add a north arrow and a scale? Maybe you can try to use a different font color. The years of the images are hard to see.

- **Author's response:**

Thanks for the reviewer's suggestion. We have added north arrows and scalebars in all sub-figures, and changed all the texts in to yellow to make it easier to recognize.

- **Author's changes in manuscript:**

We replaced the figure with a new one.

Figure 9: c) Which distance is presented on the x-axis? distance from the outlet?

- **Author's response:**

The x-axis in figure c represents the distance from P1 to P2 (i.e., the farthest end of the alluvial fan) along the main channel in Figure a-1. NOTE: To distinguish

them from T1 and T2 in Figure 5, we have modified the original labels in Figure a-1 to P1 and P2, respectively.

- **Author's changes in manuscript:**

We changed the “T1” and “T2” into “P1” and “P2” in both figure and figure caption.

Figure 11: Could you please extend the cross-section before the bridge to include the deposition areas? You could also include some information on the deposited particle sizes to exemplify.

- **Author's response:**

Following your feedback, we have the cross-section before the bridge to include the deposition areas. As shown in Figure 10c, the left bank edge of the channel has significant deposition, while the right bank platform actually has some fine particles or slurry deposited, but the graphic result is weak erosion, which may be due to the bias between the two phases of DSM. Due to the limitation of DOM resolution and the fact that debris flow slurry and particles with small size are mainly deposited in this area, particles with particles smaller than 50cm are difficult to be separated from DOM, and only a few coarse particles with size > 50cm are detected on the left bank edge, which are not enough to support our further analysis.

- **Author's changes in manuscript:**

We replaced the figure with a new one.

Line 341. The maximum erosive depth of 20.47m is in the main channel or correspond to lateral erosion? Please include the mean erosive depth at the channel.

- **Author's response:**

The maximum erosive depth of 20.47m is in the main channel. The mean erosive depth at the channel is 4.17m (The calculation area is the upstream area of the Zhibai bridge as shown in Figure 10).

- **Author's changes in manuscript:**

We add the description of mean erosive depth in manuscript.

Line 346. Could you please discuss how much underestimated is the volume you are presenting compared to Peng et al., (2022) and what is the expected error from the photogrammetric workflow?

- **Author's response:**

Our estimated final deposit volume is $12.8 \times 10^4 \text{ m}^3$, with an uncertainty of $\pm 0.493 \text{ m}$ according to DoD, and the uncertainty of deposit volume is $\pm 1.85 \times 10^4 \text{ m}^3$. Peng et al., (2022) estimated the final deposit volume is $37.5 \times 10^4 \text{ m}^3$, and our result is 65.8% smaller than Peng et al., (2022). It is noteworthy that our DSMs were derived from data collected in September, during a period of high water levels in the Yarlung Tsangpo River. This situation could result in the neglect of certain sediment, potentially submerged by the water. In contrast, Peng et al.,

(2022) utilized data from December, a time characterized by low water levels in the Yarlung Tsangpo River. During this period, previously submerged sediments became exposed, and the area of the deposit, as delineated by Chen et al., was nearly twice the size of ours. This discrepancy accounts for the primary reason behind the underestimation of volume in our study. Furthermore, Peng et al. utilized data from the Ziyuan-3 satellite, which has a coarse resolution (2.5m). This lower resolution may also impact volume estimations.

- **Author's changes in manuscript:**

We have included the above discussions in the end the 2nd paragraph of section 4.2.3.

Figure 12: The figure is not referenced in the text. Maybe you can merge Figure 12 and Figure 9 and include the location of the on-site sample.

- **Author's response:**

Thanks for the reviewer's suggestion. We have included the graph of Cumulative grain size distribution into figure 8, and numbered it as figure d. The location of the on-site sample was marked in figure 8a-1. We referenced the figure 8d in the 2nd paragraph of section 4.2.3.

- **Author's changes in manuscript:**

We deleted figure 12, and replaced the figure8 with a new one.

Figure 13: Can you add a north arrow?

- **Author's response:**

Thanks for the reviewer's suggestion. We added the scale-bars and the north arrows in the Figure.

- **Author's changes in manuscript:**

We replaced the figure with a new one.

Figure 14: Could you also include in Figure d) the other 4 debris flows for comparison?

- **Author's response:**

Thanks for the reviewer's suggestion. We have added the other 4 debris flows in Figure d for comparison.

- **Author's changes in manuscript:**

We replaced the figure with a new one.

Figures:

We have updated the figures in the manuscript, and the revised figures are as follow:

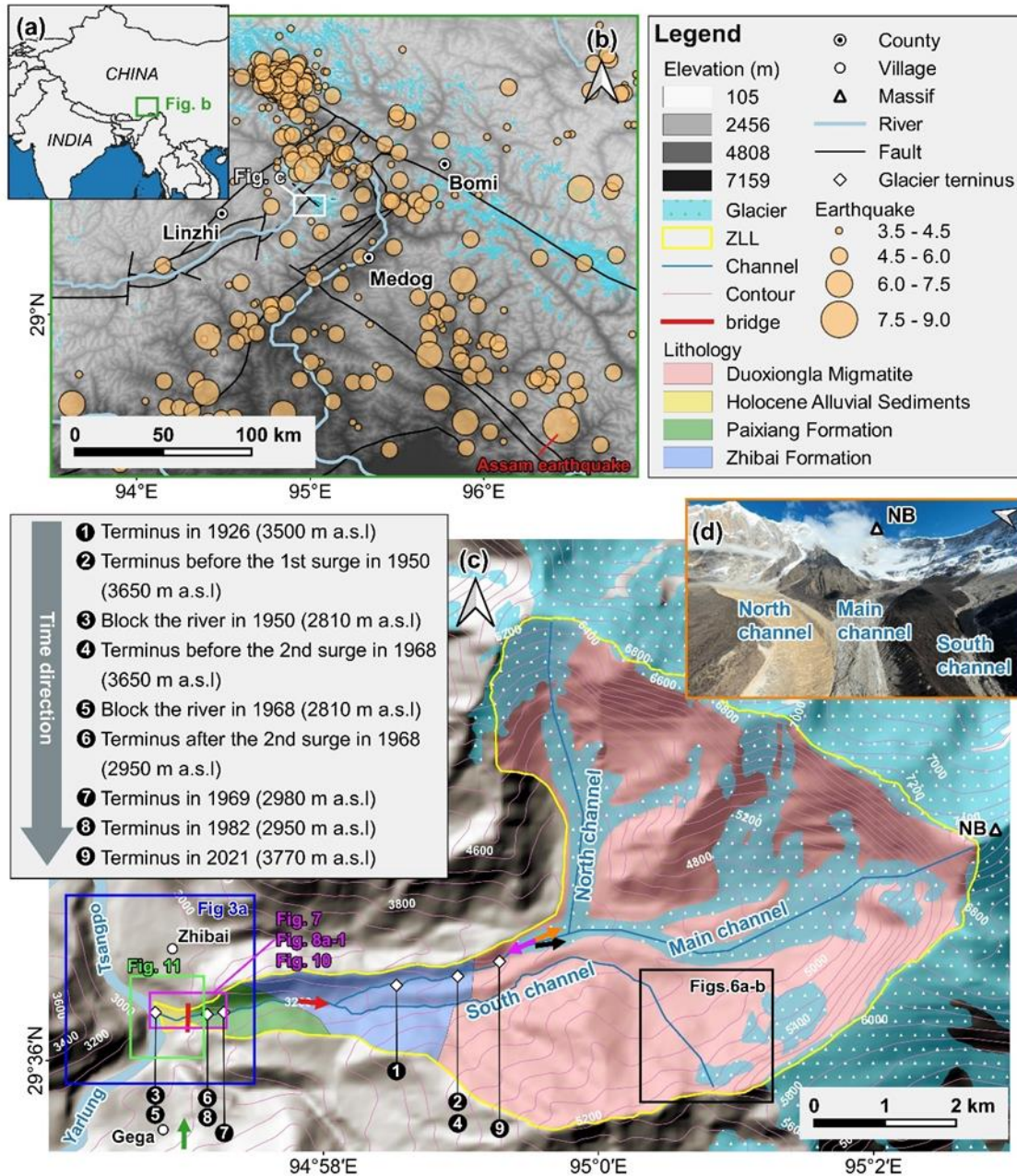


Figure 1: (a) Regional overview map of southeastern Tibet. (b) Regional settings and historical earthquakes of southeastern Tibet. (c) Topographic, geological and glacier terminus change maps of the Zelunglung catchment (the lithology refers to (Zhang and Shen, 2011)). The orange, rose-red,

green, black and red coloured arrows represent the view angle direction of figures 1d, 4, 5, 6c and 6d. (d) Aerial photo of the Zelunglung glacier and channels on December 21, 2022 (NB denotes the Namche Barwa massif).

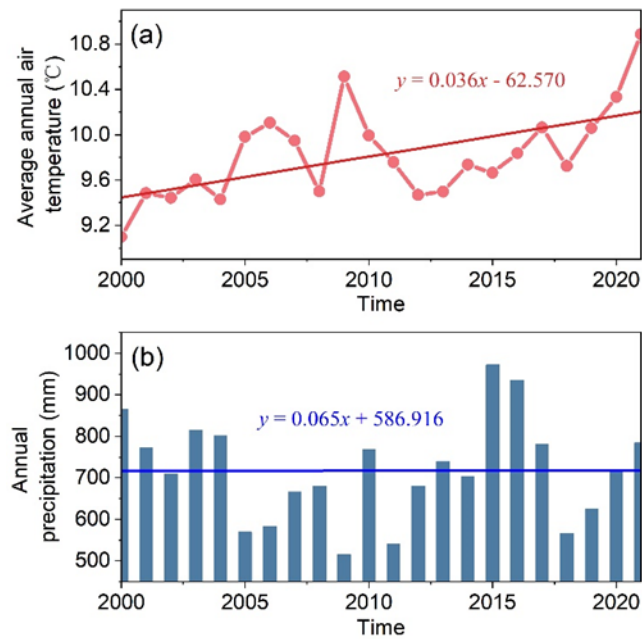


Figure 2: Annual temperature and precipitation data from 2000 to 2021 at Linzhi Meteorological Station. (Data source: <https://www.ncei.noaa.gov/maps/annual/>).

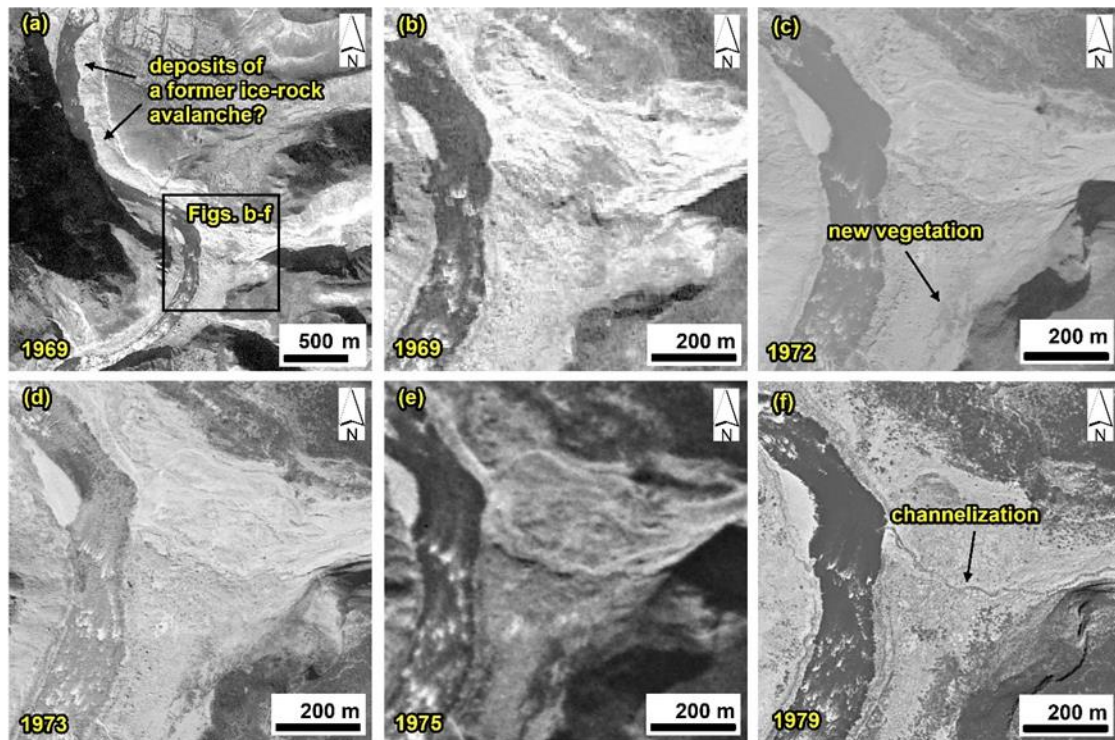


Figure 3: Variations of the Zelunglung alluvial fan during 1969 – 1979. The images are taken from Keyhole reconnaissance satellites (<https://earthexplorer.usgs.gov/>).



Figure 4: Aerial photo of the Zelunglung main channel on December 21,

2022, and the old deposits in Zhibai gully left by the 1950 event (the view angle direction is denoted by green arrow in figure 1c, and the dashed rectangle indicates the location of Figure 5b).



Figure 5: Two terraces on the banks of the main river. (a) Century Space's satellite image on 9 February 2021. (b) Picture of the terraces on the opposite bank of the Zelunglung taken on 8 September 2020. (T1 and T2 represent the terraces formed in two different periods. The green arrow denotes the view angle direction of figure b)

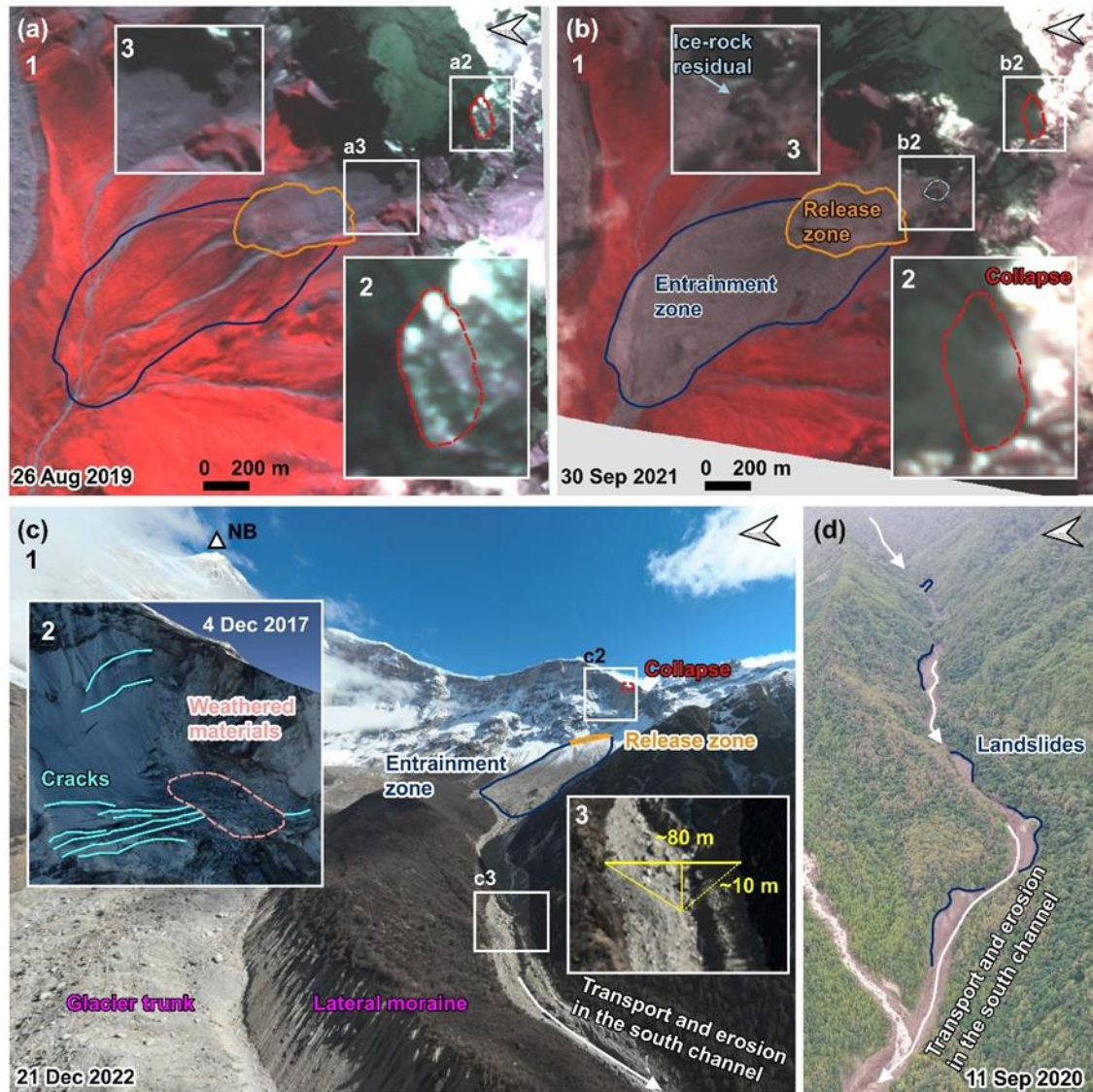


Figure 6: The initiation and propagation of the "9.10" Zelunglung periglacial glacier debris flow. (a) The planet image of the initiation area before the event. (a2) enlarged region over the pre-collapse site. (a3) Enlarge the region over the hillslope before the collapse. (b) The planet image of the initiation area after the event. (b2) enlarged region over the post-collapse site. (b3) enlarged region over the hillslope after the collapse. (base data of a-b: © 2024 Planet Labs PBC) (c) An aerial photo of the source area and the south channel on 21 December 2022 was taken by the UAV (the view angle

direction is denoted by black arrow in figure 1c). (c2) Google Earth imagery of the initiation area on 2 December 2017 (base data: ©Google Earth). (c3) The region was enlarged over the south channel on 21 December 2022. (d) An aerial photo of the downstream channel on 11 September 2020 was taken by the UAV (the view angle direction is denoted by red arrow in figure 1c).

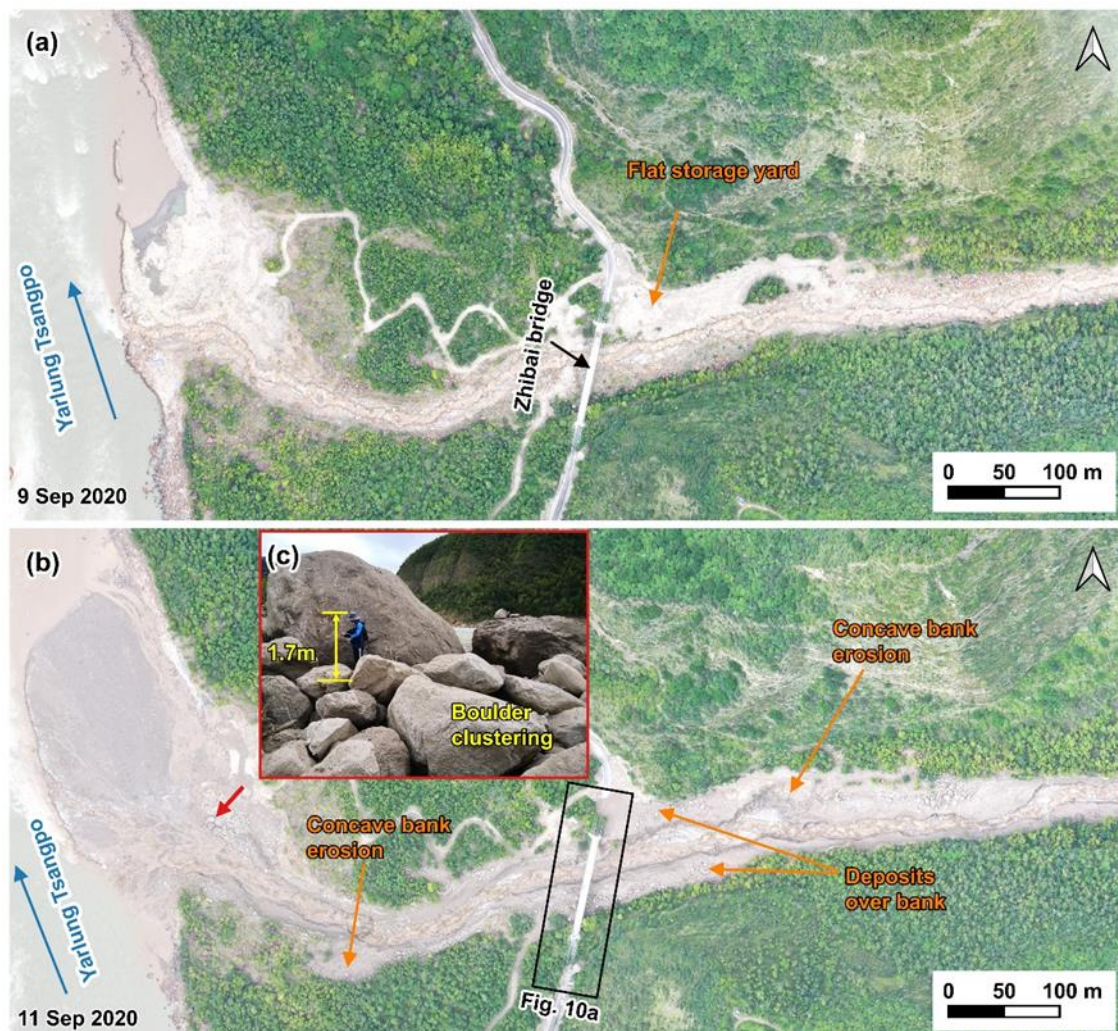


Figure 7: Comparison of pre-and post-event aerial photos on the downstream channel and alluvial fan. (a) the UAV photo on 9 September

2020; (b) the UAV photo on 11 September 2020; (c) On-site picture of the boulder clustering on 11 September 2020 (the view angle direction is denoted by red arrow in figure b).

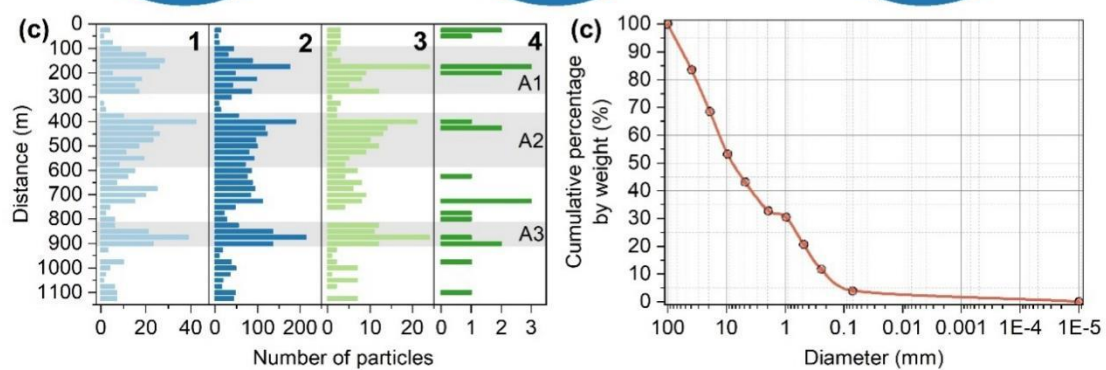
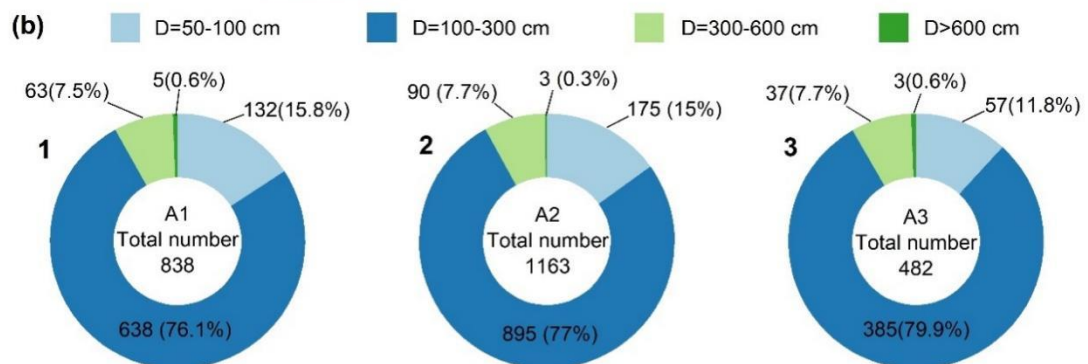
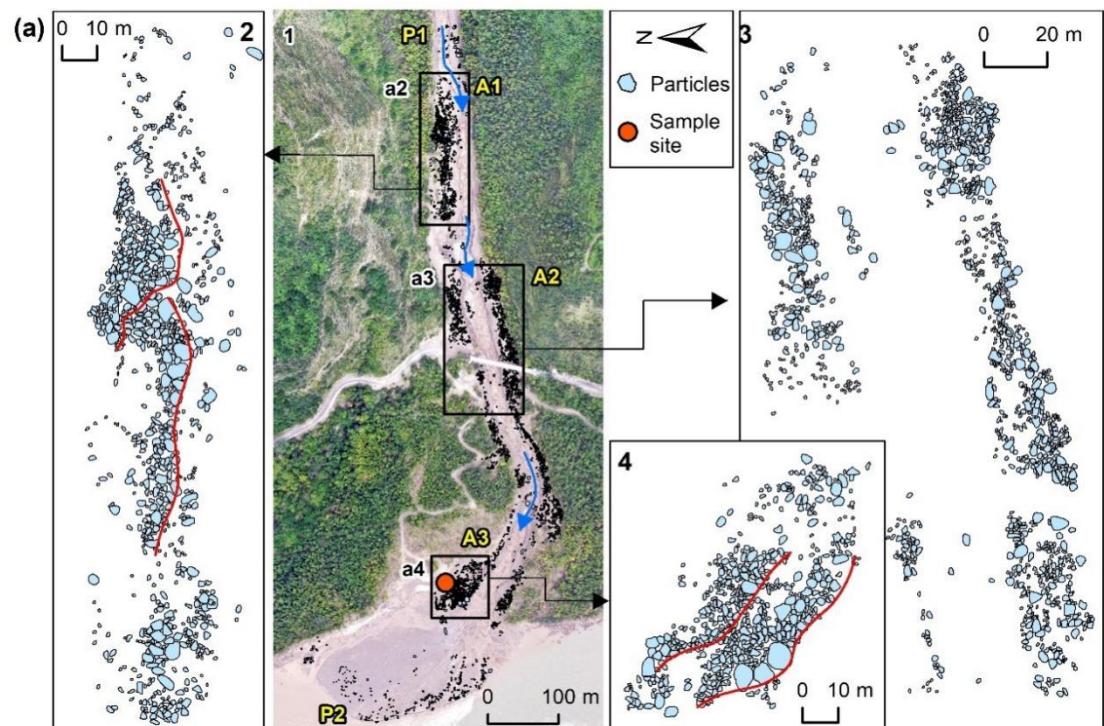


Figure 8: Distribution of the grain size. (a) The distribution of coarse particles along the channel and alluvial fan. P1 and P2 represent the places where the count starts and ends, respectively. A1-A3 are the three main deposition sites. The blue arrow is the direction of the debris flows. The bottom image is an orthographic image taken by a drone on September 10, 2020. The locations of the enlarged regions (a2)-(a4) are shown as black boxes. (a2)-(a4) enlarged region over the three main deposition sites A1-A3. Panels (b1)-(b3) show the counts of four groups of the particles in the three main deposition sites A1-A3. Panels (c1)-(c4) show the counts of four groups of the particles in the 45 segments along the channel from P1 to P2. Particles with diameters of 50-100 cm, 100-300 cm, 300-600 cm, and particles larger than 600 cm in panels b-c are shown in light blue, blue, light green, and green. (d) Cumulative grain size distribution of the on-site sample with size < 100 mm.



Figure 9: Damages to the Zhibai Bridge caused by debris flows (photos taken on 11 Sep 2020). (a) The overview of Zhibai Bridge taken by UAV and the locations shown in photographs (b)-(e) taken with handheld cameras are shown in gray circles. (b) The photo of the damaged bridge foundation. (c) The photo of the damaged steel frame. (d) Photo of on-site measurements of the vertical displacement of the bridge. (e) Photo of on-site measurements of the horizontal displacement of the bridge.

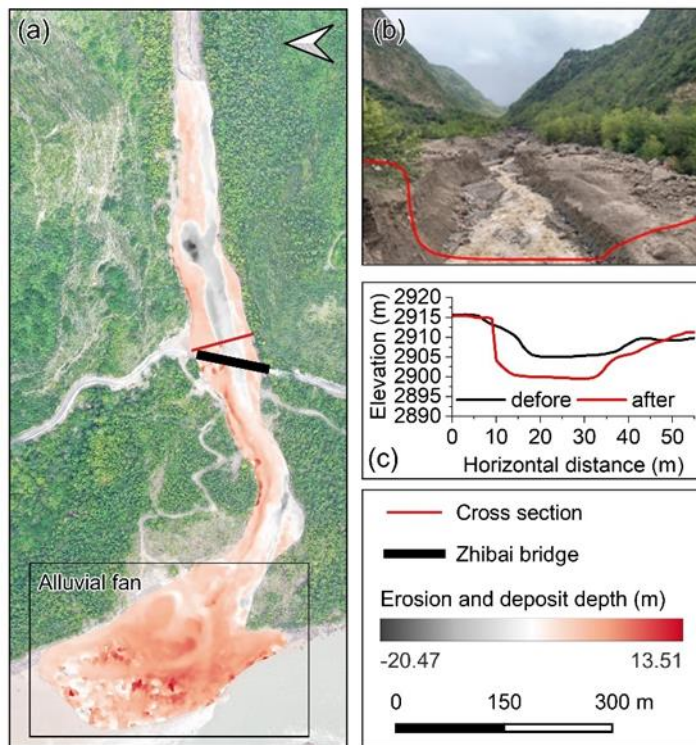


Figure 10: Geomorphic changes of the channel and alluvial fan after the debris flows of 2020. (a) Erosion and deposit depth caused by the debris flows. The base map is taken by UAV on 10 Sep 2020. (b) Photo of the channel after the debris flows. The red line represents the cross-section next to the Zhibai Bridge (photo taken on 11 Sep 2020). (c) Cross-sections

before (black) and after (red) the debris flows.

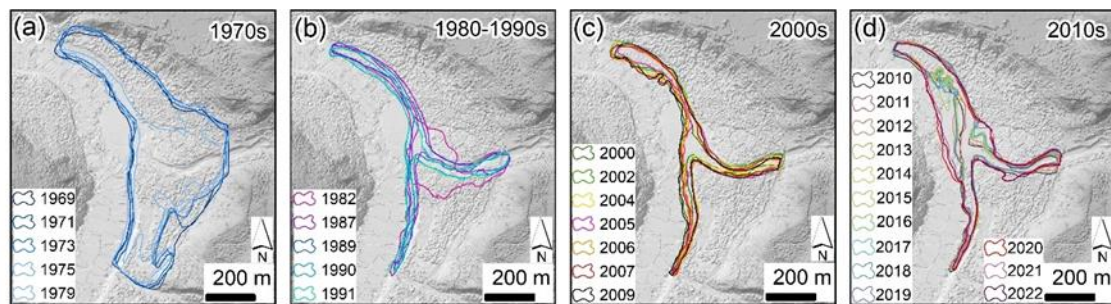


Figure 11: Evolution of the non-vegetated area in the Zelunglung alluvial fan from 1969 to 2022.

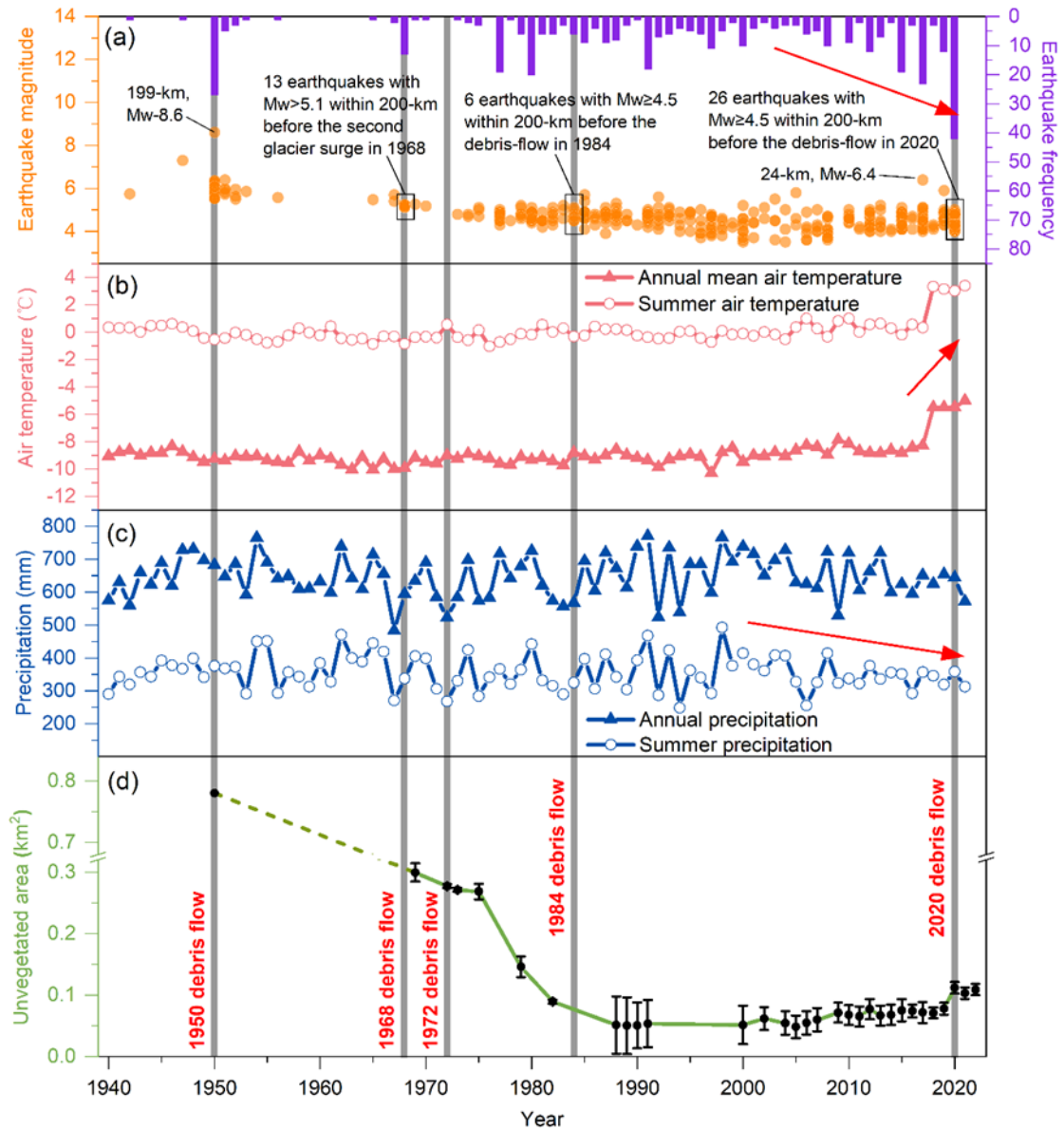


Figure 12: (a) Seismic events within a 200 km distance to the Zelunglung from 1940 to the present. (b) Changes in the annual mean and summer air temperatures in the Zelunglung from 1940 to the present. (c) Changes in the annual and summer precipitation in the Zelunglung from 1940 to the present. (d) Changes in the non-vegetated area of the Zelunglung alluvial fan from 1969 to the present (although the deposition of the 1950 event did not happen at the Zelunglung's outlet like the later events, we plot the

NVA of the 1950 event as the starting point).

Reference:

Cui, P., Wei, F. Q., He, S. M., You, Y., Chen, X. Q., Li, Z. L., Dang, C., and Yang, C. L.: Mountain Disasters Induced by the Earthquake of May 12 in Wenchuan and the Disasters Mitigation, Mountain Research, 280-282, 2008.

Dadson, S. J., Hovius, N., Chen, H., Dade, W. B., Lin, J. C., Hsu, M. L., Lin, C. W., Horng, M. J., Chen, T. C., Milliman, J., and Stark, C. P.: Earthquake-triggered increase in sediment delivery from an active mountain belt, Geology, 32, 733-736, 10.1130/g20639.1, 2004.

Dai, L. X., Scaringi, G., Fan, X. M., Yunus, A. P., Liu-Zeng, J., Xu, Q., and Huang, R. Q.: Coseismic Debris Remains in the Orogen Despite a Decade of Enhanced Landsliding, Geophysical Research Letters, 48, 10.1029/2021gl095850, 2021.

Deng, Mingfeng, Chen, Ningsheng, Liu, and Mei: Meteorological factors driving glacial till variation and the associated periglacial debris flows in Tianmo Valley, south-eastern Tibetan Plateau, Natural hazards and earth system sciences, 17, 345-356, 2017.

Du, R. H. and Zhang, S. C.: Characteristics of glacial mud-flows in South-eastern Qinghai-Xizang Plateau, Journal of Glaciology and Geocryology, 10-16+81-82, 1981.

Iverson, R. M., Schilling, S. P., and Vallance, J. W.: Objective delineation of lahar-inundation hazard zones, Geol. Soc. Am. Bull., 110, 972-984, 1998.

Kilburn, C. R. and Voight, B.: Slow rock fracture as eruption precursor at Soufriere Hills volcano, Montserrat, *Geophysical Research Letters*, 25, 3665-3668, 10.1029/98gl01609, 1998.

Parker, R. N., Densmore, A. L., Rosser, N. J., de Michele, M., Li, Y., Huang, R. Q., Whadcoat, S., and Petley, D. N.: Mass wasting triggered by the 2008 Wenchuan earthquake is greater than orogenic growth, *Nat. Geosci.*, 4, 449-452, 10.1038/ngeo1154, 2011.

Peng, D. L., Zhang, L. M., Jiang, R. C., Zhang, S., Shen, P., Lu, W. J., and He, X.: Initiation mechanisms and dynamics of a debris flow originated from debris-ice mixture slope failure in southeast Tibet, China, *Eng. Geol.*, 307, 17, 10.1016/j.enggeo.2022.106783, 2022.

Shugar, D. H., Jacquemart, M., Shean, D., Bhushan, S., Upadhyay, K., Sattar, A., Schwanghart, W., McBride, S., de Vries, M. V. W., Mergili, M., Emmer, A., Deschamps-Berger, C., McDonnell, M., Bhambri, R., Allen, S., Berthier, E., Carrivick, J. L., Clague, J. J., Dokukin, M., Dunning, S. A., Frey, H., Gascoin, S., Haritashya, U. K., Huggel, C., Kaab, A., Kargel, J. S., Kavanaugh, J. L., Lacroix, P., Petley, D., Rupper, S., Azam, M. F., Cook, S. J., Dimri, A. P., Eriksson, M., Farinotti, D., Fiddes, J., Gnyawali, K. R., Harrison, S., Jha, M., Koppes, M., Kumar, A., Leinss, S., Majeed, U., Mal, S., Muhuri, A., Noetzli, J., Paul, F., Rashid, I., Sain, K., Steiner, J., Ugalde, F., Watson, C. S., and Westoby, M. J.: A massive rock and ice avalanche caused the 2021 disaster at Chamoli, Indian Himalaya, *Science*, 373, 300-+, 10.1126/science.abh4455, 2021.

Stoffel, M.: Magnitude–frequency relationships of debris flows — A case study based on field surveys and tree-ring records, *Geomorphology*, 116, 67–76, <https://doi.org/10.1016/j.geomorph.2009.10.009>, 2010.

Tang, C., Zhu, J., Li, W. L., and Liang, J. T.: Rainfall-triggered debris flows following the Wenchuan earthquake, *Bulletin of Engineering Geology and the Environment*, 68, 187–194, 10.1007/s10064-009-0201-6, 2009.

Wang, J., Jin, Z. D., Hilton, R. G., Zhang, F., Densmore, A. L., Li, G., and West, A. J.: Controls on fluvial evacuation of sediment from earthquake-triggered landslides, *Geology*, 43, 115–118, 10.1130/g36157.1, 2015.

Wang, Z., Ma, C., Hu, K., Liu, S., and Lyu, L.: Investigation of initiation conditions of periglacial debris flows in Sanggu watershed, Eastern Himalayas, Tibet Plateau (China), *Landslides*, 20, 813–827, 10.1007/s10346-022-02003-5, 2023.

Xie, H., Zhong, D. L., Jiao, Z., and Zhang, J. S.: Debris Flow in Wenchuan Quake-hit Area in 2008, *Mountain Research*, 27, 501–509, 2009.

Zhang, J. S. and Shen, X. J.: Debris-flow of Zelongnong Ravine in Tibet, *J Mt. Sci.*, 8, 535–543, 10.1007/s11629-011-2137-0, 2011.

Zhang, X. P., Hu, K. H., Liu, S., Nie, Y., and Han, Y. Z.: Comprehensive interpretation of the Sedongpu glacier-related mass flows in the eastern Himalayan syntaxis, *J Mt. Sci.*, 19, 2469–2486, 10.1007/s11629-022-7376-8, 2022.